nature

https://doi.org/10.1038/s41586-020-2598-9

Accelerated Article Preview

SARS-CoV-2-reactive T cells in healthy donors and patients with COVID-19

Received: 9 April 2020

Accepted: 22 July 2020

Accelerated Article Preview Published online 29 July 2020

Cite this article as: Braun, J. et al. SARS-CoV-2-reactive T cells in healthy donors and patients with COVID-19. *Nature* https://doi.org/10.1038/s41586-020-2598-9 (2020).

Julian Braun, Lucie Loyal, Marco Frentsch, Daniel Wendisch, Philipp Georg, Florian Kurth, Stefan Hippenstiel, Manuela Dingeldey, Beate Kruse, Florent Fauchere, Emre Baysal, Maike Mangold, Larissa Henze, Roland Lauster, Marcus A. Mall, Kirsten Beyer, Jobst Röhmel, Sebastian Voigt, Jürgen Schmitz, Stefan Miltenyi, Ilja Demuth, Marcel A. Müller, Andreas Hocke, Martin Witzenrath, Norbert Suttorp, Florian Kern, Ulf Reimer, Holger Wenschuh, Christian Drosten, Victor M. Corman, Claudia Giesecke-Thiel, Leif Erik Sander & Andreas Thiel

This is a PDF file of a peer-reviewed paper that has been accepted for publication. Although unedited, the content has been subjected to preliminary formatting. Nature is providing this early version of the typeset paper as a service to our authors and readers. The text and figures will undergo copyediting and a proof review before the paper is published in its final form. Please note that during the production process errors may be discovered which could affect the content, and all legal disclaimers apply.

ACCELERATED ARTICLE PREVIEW

Article

SARS-CoV-2-reactive T cells in healthy donors and patients with COVID-19

https://doi.org/10.1038/s41586-020-2598-9

Received: 9 April 2020

Accepted: 22 July 2020

Published online: 29 July 2020

Julian Braun[1,2,16], Lucie Loyal[1,2,16], Marco Frentsch[3,16], Daniel Wendisch[4], Philipp Georg[4], Florian Kurth[4,5], Stefan Hippenstiel[4], Manuela Dingeldey[1,2], Beate Kruse[1,2], Florent Fauchere[1,2], Emre Baysal[1,2], Maike Mangold[1,2], Larissa Henze[1,2], Roland Lauster[1,6], Marcus A. Mall[7,13], Kirsten Beyer[7], Jobst Röhmel[7], Sebastian Voigt[8], Jürgen Schmitz[9], Stefan Miltenyi[9], Ilja Demuth[10], Marcel A. Müller[11], Andreas Hocke[4], Martin Witzenrath[4], Norbert Suttorp[4], Florian Kern[12,13], Ulf Reimer[12], Holger Wenschuh[12], Christian Drosten[11,14], Victor M. Corman[11], Claudia Giesecke-Thiel[15,17] ✉, Leif Erik Sander[4,17] ✉ & Andreas Thiel[1,2,17] ✉

Severe acute respiratory syndrome coronavirus 2 (SARS-CoV-2) has caused the rapidly unfolding coronavirus disease 2019 (COVID-19) pandemic[1,2]. Clinical manifestations of COVID-19 vary, ranging from asymptomatic infection to respiratory failure. The mechanisms determining such variable outcomes remain unresolved. Here, we investigated SARS-CoV-2 spike glycoprotein (S)-reactive $CD4^+$ T cells in peripheral blood of patients with COVID-19 and SARS-CoV-2-unexposed healthy donors (HD). We detected SARS-CoV-2 S-reactive $CD4^+$ T cells in 83% of patients with COVID-19 but also in 35% of HD. S-reactive $CD4^+$ T cells in HD reacted primarily to C-terminal S epitopes, which show a higher homology to spike glycoproteins of human endemic coronaviruses, compared to N-terminal epitopes. S-reactive T cell lines generated from SARS-CoV-2-naive HD responded similarly to C-terminal S of human endemic coronaviruses 229E and OC43 and SARS-CoV-2, demonstrating the presence of S-cross-reactive T cells, probably generated during past encounters with endemic coronaviruses. The role of pre-existing SARS-CoV-2 cross-reactive T cells for clinical outcomes remains to be determined in larger cohorts. However, the presence of S-cross-reactive T cells in a sizable fraction of the general population may affect the dynamics of the current pandemic, and has important implications for the design and analysis of upcoming COVID-19 vaccine trials.

The COVID-19 pandemic poses an unprecedented threat to public health and the global economy with ever-increasing cases and COVID-19-related deaths worldwide[1,2]. COVID-19 is routinely diagnosed by detection of SARS-CoV-2 RNA in nasopharyngeal swabs via PCR[3], which works reliably in the acute phase of COVID-19[4,5]. However, limited test availability and preferential testing of symptomatic patients has likely lead to significant underestimation of infection burden and overestimation of case-fatality rates[6]. Serological analysis of SARS-CoV-2-induced humoral immunity could reveal asymptomatic infections, but it is not yet widely applied[7,8] and complicated by the fact that coronavirus-induced antibody responses are quite variable and rather short-lived[9,10]. Coronavirus-induced cellular immunity is predicted to be more sustained, but poorly characterized so far. However, several T cell epitopes in coronavirus structural proteins have been predicted or identified[9,11–13]. Importantly, T helper cell responses and generation of neutralizing antibodies may be interdependent[9,14]. Studies of the SARS-CoV epidemic in 2002/03 have shown that adaptive immune responses directed against spike glycoprotein were protective[9,15,16]. Hence, induction of SARS-CoV-2-specific $CD4^+$ T cells is likely to be critical in the instruction of affinity maturated and potentially protective antibody responses[17]. We therefore examined the presence, frequencies and phenotypic characteristics of SARS-CoV-2 spike glycoprotein (S)-reactive T cells in COVID-19 patients compared to SARS-CoV-2 unexposed healthy donors (HD).

Identification of S-reactive $CD4^+$ T cells

We identified S-reactive $CD4^+$ T cells by flow cytometry according to their expression of CD40L and 4-1BB after *in vitro* stimulation with S

[1]Si-M / 'Der Simulierte Mensch', Technische Universität Berlin and Charité–Universitätsmedizin Berlin, Berlin, Germany. [2]Regenerative Immunology and Aging, BIH Center for Regenerative Therapies, Charité–Universitätsmedizin Berlin, Berlin, Germany. [3]Department of Hematology, Oncology and Tumor Immunology, Charité–Universitätsmedizin Berlin, Berlin, Germany. [4]Department of Infectious Diseases and Respiratory Medicine, Charité–Universitätsmedizin Berlin, Berlin, Germany. [5]Department of Tropical Medicine, Bernhard Nocht Institute for Tropical Medicine and I. Department of Medicine, University Medical Center Hamburg–Eppendorf, Hamburg, Germany. [6]Medical Biotechnology, Institute for Biotechnology, Technische Universität Berlin, Berlin, Germany. [7]Department of Pediatric Pulmonology, Immunology and Critical Care Medicine, Charité - Universitätsmedizin Berlin, Berlin, Germany. [8]Robert Koch Institut, Berlin, Germany. [9]Miltenyi Biotec, Bergisch Gladbach, Germany. [10]Interdisciplinary Metabolism Center, Biology of Aging (BoA) group, Charité–Universitätsmedizin Berlin, Berlin, Germany. [11]Institute of Virology, Charité–Universitätsmedizin Berlin, Berlin, Germany. [12]JPT Peptide Technologies GmbH, Berlin, Germany. [13]Brighton and Sussex Medical School, Department of Clinical and Experimental Medicine, Brighton, UK. [14]Berlin Institute of Health (BIH), Berlin, Germany. [15]Max Planck Institute for Molecular Genetics, Berlin, Germany. [16]These authors contributed equally: Julian Braun, Lucie Loyal, Marco Frentsch. [17]These authors jointly supervised this work: Claudia Giesecke-Thiel, Leif Erik Sander, Andreas Thiel. ✉e-mail: giesecke@molgen.mpg.de; leif-erik.sander@charite.de; andreas.thiel@charite.de

ACCELERATED ARTICLE PREVIEW

peptides. To this end, we designed two peptide pools (15 amino acids (aa), 11 aa overlaps) spanning the entire S that comprised different amounts of putative MHC-II epitopes based on identified epitopes in SARS-CoV[11–13] (Fig. 1a). SARS-CoV-2 S peptide pool PepMix™ 1 (henceforth: S-I) spans the N-terminal part (aa residues 1-643) including 21 predicted SARS-CoV MHC-II epitopes (Fig. 1a, Extended Data Fig. 1, Extended Data Table 1). The second peptide pool PepMix™ 2 (S-II) covered the C-terminal portion (amino acid residues 633-1273) including 13 predicted SARS-CoV MHC-II epitopes (Fig. 1a, Extended Data Fig. 1, Extended Data Table 1). The peptides of the receptor-binding domain (RBD) in the subunit S1, which represents a major target of neutralizing antibodies, are included in S-I[18,19].

For antigen-specific stimulation, PBMC from patients and HD (see patient and HD characteristics: Table 1, Extended Data Table 2 and 3) were stimulated for 16 hours with S-I and S-II peptide pools, respectively. Antigen-reactive CD4$^+$ T cells were identified by co-expression of 4-1BB and CD40L, which allows for sensitive detection of S-reactive CD4$^+$ T cells re-activated by TCR engagement *ex vivo*[20–22] (Fig. 2a, Extended Data Fig. 2, and Supplementary File). In 12 (67%) and 15 (83%) of 18 patients we detected CD4$^+$ T cells reacting against the S-I and the S-II peptide pool, respectively (Fig. 2b, d, e). Most COVID-19 patients with critical disease exhibited no reactivity to S-I (Extended Data Fig. 3).

Remarkably, S-II-reactive CD4$^+$ T cells, albeit at slightly lower frequencies compared with patients, could also be detected in 24 of 68 HD (35%), henceforth referred to as reactive healthy donors (RHD) (Fig. 2c, d, e). S-I-reactive CD4$^+$ T cells could only be detected in 6 out of the 24 RHD, i.e. in 5.8% of all HD (Fig. 2d, e). All HD were negative for IgG antibodies specific for S subunit 1 (S1) in contrast to patients (Fig. 2f). We further ruled out early SARS-CoV-2 infection at initial sampling by 1) direct PCR standard diagnosis in 10 RHD (data not shown), 2) serological testing (Fig. 2f) and 3) by repeated serological testing at least 28 days later for 65 of 68 HD (Extended Data Fig. 4).

We further phenotypically and functionally characterized S-reactive CD4$^+$ T cells in additional patients (Extended Data Table 4) and RHD. Notably, in both groups, SARS-CoV-2 S-II-reactive CD4$^+$ T cells exhibited a memory phenotype and a significant proportion of the cells expressed IFNγ, indicative of T_H1 polarization (Fig. 2g, Extended Data Fig. 5a-d). Most S-reactive CD4$^+$ T cells expressed IL-2 but only few expressed IL-17A (Extended Data Fig. 5a-d). Frequencies of S-II-reactive CD4$^+$ T cells expressing IFNγ$^+$ were similar in patients and RHD (Fig. 2g). Testing for TNFα expression revealed that S-II reactive IFNγ$^+$ CD4$^+$ T cells from RHD mostly co-expressed TNFα, whereas S-II reactive IFNγ$^+$ CD4$^+$ T cells from P displayed rather heterogenous TNFα expression patterns (Extended Data Figure 5e). This is likely reflecting the different disease stages during the acute SARS-CoV-2 infection of the individual patients included in our study. These results demonstrate the presence of S-reactive CD4$^+$ T cells with a predominantly T_H1 memory phenotype not only in COVID-19 patients but also in seronegative SARS-CoV-2 unexposed HD.

S-reactive CD4$^+$ T cells in RHD are cross-reactive to HCoVs 229E and OC43

S-reactive CD4$^+$ T cells from COVID-19 patients equally targeted both, the N-terminal (S-I) and C-terminal peptide pools (S-II) of S, while S-reactive CD4$^+$ T cells from RHD reacted significantly stronger to S-II (Fig. 2d). S-II exhibits a higher homology to human endemic "common cold" coronaviruses (HCoVs) 229E, NL63, OC43, and HKU1 with regard to the SARS-CoV MHC-II epitopes, as compared to peptide pool S-I (Extended Data Table 1 and Extended Data Fig. 1). This suggests that S-reactivity in SARS-CoV-2 naïve HD originated from previous immune responses to HCoVs. We therefore tested 18 of the 68 HD for the presence of antibodies specific for the four endemic HCoVs. We detected IgG antibodies against all four HCoVs in all tested HD, regardless of the presence of measurable S-reactive CD4$^+$ T cells (Extended Data Fig. 6a). Frequencies of S-(cross)-reactive CD4$^+$ T cells in RHD did not correlate with antibody levels against HCoVs potentially indicating that they have not been generated very recently. Similar findings have been obtained for other anti-viral CD4$^+$ T cell responses, for example following yellow fever vaccination (YFV-17D). CD4$^+$ T cell responses showed a significant correlation with the later generation of high titers of neutralizing antibodies only at very early time points after YFV-17D vaccination[23].

We next determined whether SARS-CoV-2 S-reactive CD4$^+$ T cells in RHD correlated with a CD4$^+$ T cell response to spike glycoprotein of endemic HCoVs (S_{HCoV}). To this end, PBMC from HD and RHD were stimulated with S-I and S-II pools from SARS-CoV-2 and S_{HCoV}-I and S_{HCoV}-II (spike gylcoprotein subunit 1 and subunit 2 peptide pool, respectively) of OC43 and 229E (Fig. 2h, and Extended Data Fig. 6b-d), respectively. There was a strong positive correlation of CD4$^+$ T cell reactivity against S-II and S_{HCoV}-II of OC43 and 229E (r=0.629, r=0.715, Fig. 2h), respectively, while there was no or only a weak negative correlation detected between S-I-reactivity and reactivity towards S_{HCoV}-I of OC43 and 229E, respectively (r=0.037, r=-0.259) (Extended Data Fig. 6b). No correlation was observed between reactivity towards S-I/S-II and CMVpp65 (Extended Data Fig. 6c, d).

Next, we tested whether S-reactive CD4$^+$ T cells of RHD responded to stimulation with S_{HCoV}. To this end, from three RHD (RHD01, 07 and 15), S-II-reactive CD4$^+$ T cells were isolated, expanded *ex vivo* for 12 days and subsequently re-stimulated with S_{HCoV}-I and S_{HCoV}-II of OC43 and 229E, with the S-II pool as positive control, and S-I and a peptide pool from CMVpp65 as negative controls (Fig. 2i, j). Restimulation with the SARS-CoV-2 S-II peptide pool induced the highest frequencies of 4-1BB$^+$CD40L$^+$ CD4$^+$ T cells, while negligible responses were measured in the negative controls (S-I, CMVpp65, unstimulated), demonstrating the high specificity of the established S-II reactive CD4$^+$ T cell lines (Fig. 2j). In contrast, strong responses were observed against S_{HCoV}-II peptide pools of the two HCoVs (Fig. 2j). These findings provide evidence that cross-reactivity of SARS-CoV-2 S-II-reactive cells to S_{HCoV} in the tested RHD, suggesting that pre-existence of SARS-CoV-2 reactive T cells in seronegative naïve individuals originates from prior immune responses to endemic HCoVs.

Specific activation signatures in COVID-19 patients

Finally, we assessed additional activation marker profiles on S-reactive T cells from COVID-19 patients and RHD. Expression of CD38, HLA-DR and Ki-67 has previously been shown to reliably characterize recently *in vivo* activated human T cells during acute and chronic infection[24–28]. Notably, S-reactive CD4$^+$ T cells from patients largely expressed CD38, HLA-DR and Ki-67 (Fig. 3a–d). The majority of S-reactive T cells in patients co-expressed CD38 and HLA-DR (Fig. 3e), characteristic for effector T cell responses during acute viral infections[24,26], whereas CD38 and Ki-67 co-expression was more variable (Fig. 3f). By contrast, S-reactive CD4$^+$ T cells from RHD did not express CD38, HLA-DR and Ki-67, or only at low frequencies (Fig. 3b–f), and co-expression was not observed (Fig. 3e, f). In patients, considerable proportions of the entire peripheral CD4$^+$ and CD8$^+$ T cell populations co-expressed CD38 and HLA-DR (data not shown), which, however, could not be re-activated with our S peptide pools *in vitro*. These findings are in line with results of a recent study showing refractory T cell signatures in COVID-19 patients[29]. Additionally, a proportion of these CD38$^+$HLADR$^+$ CD4$^+$ T cells likely targets other structural proteins of SARS-CoV-2. We furthermore show that the presence of S-reactive CD4$^+$ T cells and in particular of CD38-expressing cells among S-reactive CD4$^+$ T cells exhibited a high variability among patients in the course of COVID-19 disease (Fig. 3g, h).

Discussion

Our study demonstrates the presence of S-reactive CD4$^+$ T cells in COVID-19 patients, and in a considerable proportion of SARS-CoV-2

ACCELERATED ARTICLE PREVIEW

unexposed HD. In light of the recent emergence of SARS-CoV-2, our data raise the intriguing possibility that such pre-existing S-reactive T cells represent cross-reactive clones, probably acquired in previous infections with endemic HCoVs. HCoVs account for approximately 20% of "common cold" upper respiratory tract infections, are ubiquitous, but display a winter seasonality[30–32]. Based on epidemiological data, it may be extrapolated that adults contract an HCoV infection on average every two to three years. Protective antibodies may wane mid-term but cellular immunity could remain[13,33]. Although the overall amino acid sequence homology of S is relatively low compared to spike glycoproteins of HCoVs, there is an overlap of MHC-II epitopes especially in the C-terminal domain of the here used peptide pools (Fig. 1a, Extended Data Fig. 1). This may explain the preferential reactivity of $CD4^+$ T cells to the C-terminal domain in one third of HD.

The biological role of pre-existing S-cross-reactive $CD4^+$ T cells in 35% of HD remains unclear for now. However, assuming that these cells have a protective role in SARS-CoV-2 infection, they may contribute to understanding the divergent manifestations of COVID-19, and the striking resilience of children and young adults to symptomatic SARS-CoV-2 infection. Especially children in day care centers but also young adults have more frequent social contacts than elderly, and thus may have a higher HCoV prevalence. This hypothesis requires further investigation in future longitudinal studies assessing the presence of pre-existing SARS-CoV-2-cross-reactive $CD4^+$ T cells and their impact on the susceptibility to SARS-CoV-2 infection and age-related clinical outcomes of COVID-19.

SARS-CoV neutralizing antibodies are associated with convalescence, and they have been detected 12 months after disease[9]. However, the durability of neutralizing antibody responses against SARS-CoV-2 remains unknown. Although antibodies against HCoV can wane within months after infection, HCoV re-infection is accompanied by low-level and short-lived virus shedding with only mild symptoms of short duration pointing towards humoral-independent residual immunity[10]. Cellular immunity has not yet been studied in this context. In mouse models, however, $CD4^+$ as well as $CD8^+$ T cell responses directed against structural proteins such as spike or nucleocapsid protein of SARS-CoV critically contributed to viral clearance[15,34,35]. Understanding the extent to which and how SARS-CoV-2-specific humoral or cellular immunity mediates durable protection against reinfection is of critical importance in the coming months.

Our study reveals pre-existing cellular SARS-CoV-2-cross-reactivity in a substantial proportion of SARS-CoV-2 seronegative HD. This finding might have significant epidemiological implications regarding herd immunity thresholds and projections for the COVID-19 pandemic. Our results provide a decisive rationale to initiate worldwide prospective studies to assess the contribution of pre-existing, potentially region-dependent SARS-CoV-2-cross-reactive immunity to the diverse clinical outcomes of SARS-CoV-2 infections. Together with currently introduced novel serological tests, the data generated by such studies may critically inform evidence-based risk evaluation, patient monitoring, adaptation of containment methods, and last but not least, vaccine development.

Online content

Any methods, additional references, Nature Research reporting summaries, source data, extended data, supplementary information, acknowledgements, peer review information; details of author contributions and competing interests; and statements of data and code availability are available at https://doi.org/10.1038/s41586-020-2598-9.

1. Dong, E., Du, H. & Gardner, L. COVID-19 in real time. *Lancet Infect. Dis.* **3099**, 19–20 (2020).
2. Wang, D. *et al*. Clinical Characteristics of 138 Hospitalized Patients with 2019 Novel Coronavirus-Infected Pneumonia in Wuhan, China. *JAMA - J. Am. Med. Assoc.* (2020). https://doi.org/10.1001/jama.2020.1585
3. Corman, V. M. *et al*. Detection of 2019 novel coronavirus (2019-nCoV) by real-time RT-PCR. *Euro Surveill.* (2020). https://doi.org/10.2807/1560-7917.ES.2020.25.3.2000045
4. Loeffelholz, M. J. & Tang, Y.-W. Laboratory diagnosis of emerging human coronavirus infections – the state of the art. *Emerg. Microbes Infect.* **9**, 747–756 (2020).
5. Wölfel, R. *et al*. Virological assessment of hospitalized patients with COVID-2019. *Nature* 1–10 (2020). https://doi.org/10.1038/s41586-020-2196-x
6. Wu, J. T., Leung, K. & Leung, G. M. Nowcasting and forecasting the potential domestic and international spread of the 2019-nCoV outbreak originating in Wuhan, China: a modelling study. *Lancet* **395**, 689–697 (2020).
7. Amanat, F. *et al*. A serological assay to detect SARS-CoV-2 seroconversion in humans. *medRxiv* 2020.03.17.20037713 (2020). https://doi.org/10.1101/2020.03.17.20037713
8. Okba, N. M. A. *et al*. SARS-CoV-2 specific antibody responses in COVID-19 patients. *medRxiv* 2020.03.18.20038059 (2020). https://doi.org/10.1101/2020.03.18.20038059
9. Li, C. K. *et al*. T Cell Responses to Whole SARS Coronavirus in Humans. *J. Immunol.* **181**, 5490–5500 (2008).
10. Callow, K. A., Parry, H. F., Sergeant, M. & Tyrrell, D. A. J. The time course of the immune response to experimental coronavirus infection of man Nasal washings. 435–446 (1990).
11. Libraty, D. H., O'Neil, K. M., Baker, L. M., Acosta, L. P. & Olveda, R. M. Human CD4+ Memory T-lymphocyte Responses to SARS Coronavirus Infection. *Virology* **368**, 317–321 (2007).
12. Yang, J. *et al*. Searching immunodominant epitopes prior to epidemic: HLA class II-restricted SARS-CoV spike protein epitopes in unexposed individuals. *Int. Immunol.* **21**, 63—71 (2009).
13. Ng, O. *et al*. Memory T cell responses targeting the SARS coronavirus persist up to 11 years post-infection. *Vaccine* **34**, 2008–2014 (2016).
14. Mitchison, N. A. *T-cell–B-cell cooperation*. **4**, 1599–1601 (2004).
15. Yang, Z. *et al*. A DNA vaccine induces SARS coronavirus neutralization and protective immunity in mice. *Nature* **428**, 561–564 (2004).
16. Zhu, Z. *et al*. Potent cross-reactive neutralization of SARS coronavirus isolates by human monoclonal antibodies. *Proc. Natl. Acad. Sci.* **104**, 12123–12128 (2007).
17. Ju, B. *et al*. Potent human neutralizing antibodies elicited by SARS-CoV-2 infection. *bioRxiv* 2020.03.21.990770 (2020). https://doi.org/10.1101/2020.03.21.990770
18. Meng, T. *et al*. The insert sequence in SARS-CoV-2 enhances spike protein cleavage by TMPRSS. (2020).
19. Walls, A. C. *et al*. Structure, Function, and Antigenicity of the SARS-CoV-2 Spike Glycoprotein. *Cell* (2020). https://doi.org/10.1016/j.cell.2020.02.058
20. Frentsch, M. *et al*. Direct access to CD4+ T cells specific for defined antigens according to CD154 expression. *Nat. Med.* **11**, 1118–1124 (2005).
21. Sattler, A. *et al*. Cytokine-induced human IFN-γ–secreting effector-memory Th cells in chronic autoimmune inflammation. *Blood* **113**, 1948–1956 (2009).
22. Schoenbrunn, A. *et al*. A Converse 4-1BB and CD40 Ligand Expression Pattern Delineates Activated Regulatory T Cells (Treg) and Conventional T Cells Enabling Direct Isolation of Alloantigen-Reactive Natural Foxp3+ Treg. *J. Immunol.* **189**, 5985–5994 (2012).
23. Kohler, S. *et al*. The early cellular signatures of protective immunity induced by live viral vaccination. *Eur. J. Immunol.* (2012). https://doi.org/10.1002/eji.201142306
24. Appay, V. *et al*. Memory CD8+ T cells vary in differentiation phenotype in different persistent virus infections. *Nat. Med.* (2002). https://doi.org/10.1038/nm0402-379
25. Blom, K. *et al*. Temporal Dynamics of the Primary Human T Cell Response to Yellow Fever Virus 17D As It Matures from an Effector- to a Memory-Type Response. *J. Immunol.* (2013). https://doi.org/10.4049/jimmunol.1202234
26. Callan, M. F. C. *et al*. Direct visualization of antigen-specific CD8+ T cells during the primary immune response to Epstein-Barr virus in vivo. *J. Exp. Med.* **187**, 1395–1402 (1998).
27. Miller, J. D. *et al*. Human Effector and Memory CD8+ T Cell Responses to Smallpox and Yellow Fever Vaccines. *Immunity* (2008). https://doi.org/10.1016/j.immuni.2008.02.020
28. Schulz, A. R. *et al*. Low Thymic Activity and Dendritic Cell Numbers Are Associated with the Immune Response to Primary Viral Infection in Elderly Humans. *J. Immunol.* (2015). https://doi.org/10.4049/jimmunol.1500598
29. Diao, B. *et al*. Reduction and Functional Exhaustion of T Cells in Patients with Coronavirus Disease 2019 (COVID-19). *medRxiv* (2020). https://doi.org/10.1101/2020.02.18.20024364 .
30. Tyrrell, D. A. J. *Common colds and Related Diseases*. (1965).

Publisher's note Springer Nature remains neutral with regard to jurisdictional claims in published maps and institutional affiliations.

© The Author(s), under exclusive licence to Springer Nature Limited 2020

ACCEPTED ARTICLE PREVIEW

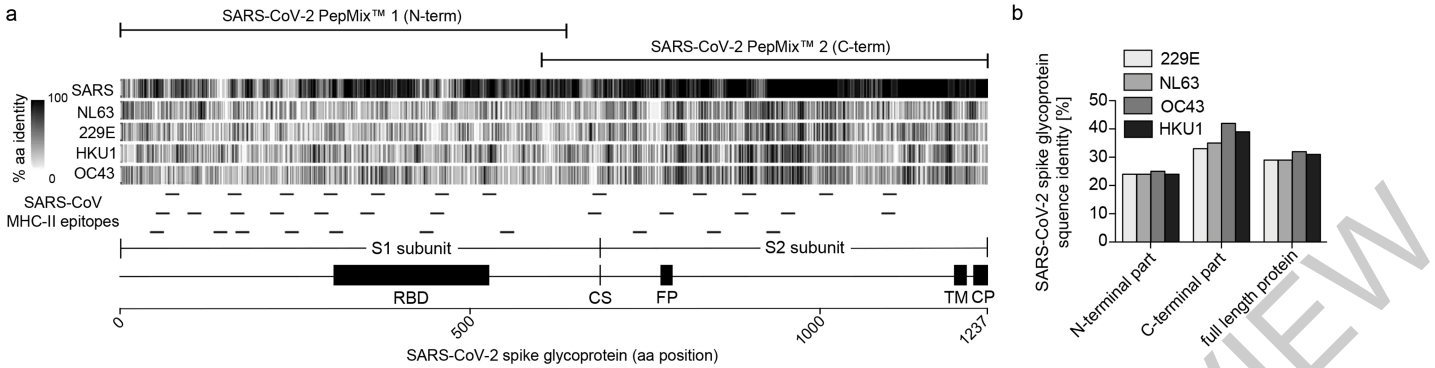

Fig. 1 | Structural domains, homology and MHC-II epitopes of the SARS-CoV-2 spike glycoprotein. a, SARS-CoV-2 spike glycoprotein (1237 amino acids (aa)) is separated at the cleavage site (CS) into subunit S1 harboring the receptor-binding domain (RBD) and subunit S2 containing the fusion peptide (FP), the transmembrane domain (TM) and the cytoplasmic peptide (CP). Sequence homology of spike glycoprotein of SARS-CoV-2 to SARS-CoV and HCoV strains NL63, 229E, HKU1 and OC43 was calculated as percentage of aa identity in sliding windows of 10 aa and is depicted as grey vertical scale bars. Predicted SARS-CoV MHC-II epitopes are indicated as small horizontal lines below and sequences and references are listed in Extended Data Table 1. Homology is depicted for each reported MHC-II epitope in Extended Data Figure 1. SARS-CoV-2 PepMix™ 1 (N-term) (in the main text referred to as S-I) spans over the N-terminal and SARS-CoV-2 PepMix™ 2 (C-term) (in the main text referred to as S-II) spans over the C-terminal part of S, as indicated above the alignment. **b**, Proportion of sequence identity of the N-terminal and C-terminal parts of SARS-CoV-2 spike glycoprotein to the spike glycoproteins of HCoV strains NL63, 229E, HKU1 and OC43.

ACCELERATED ARTICLE PREVIEW

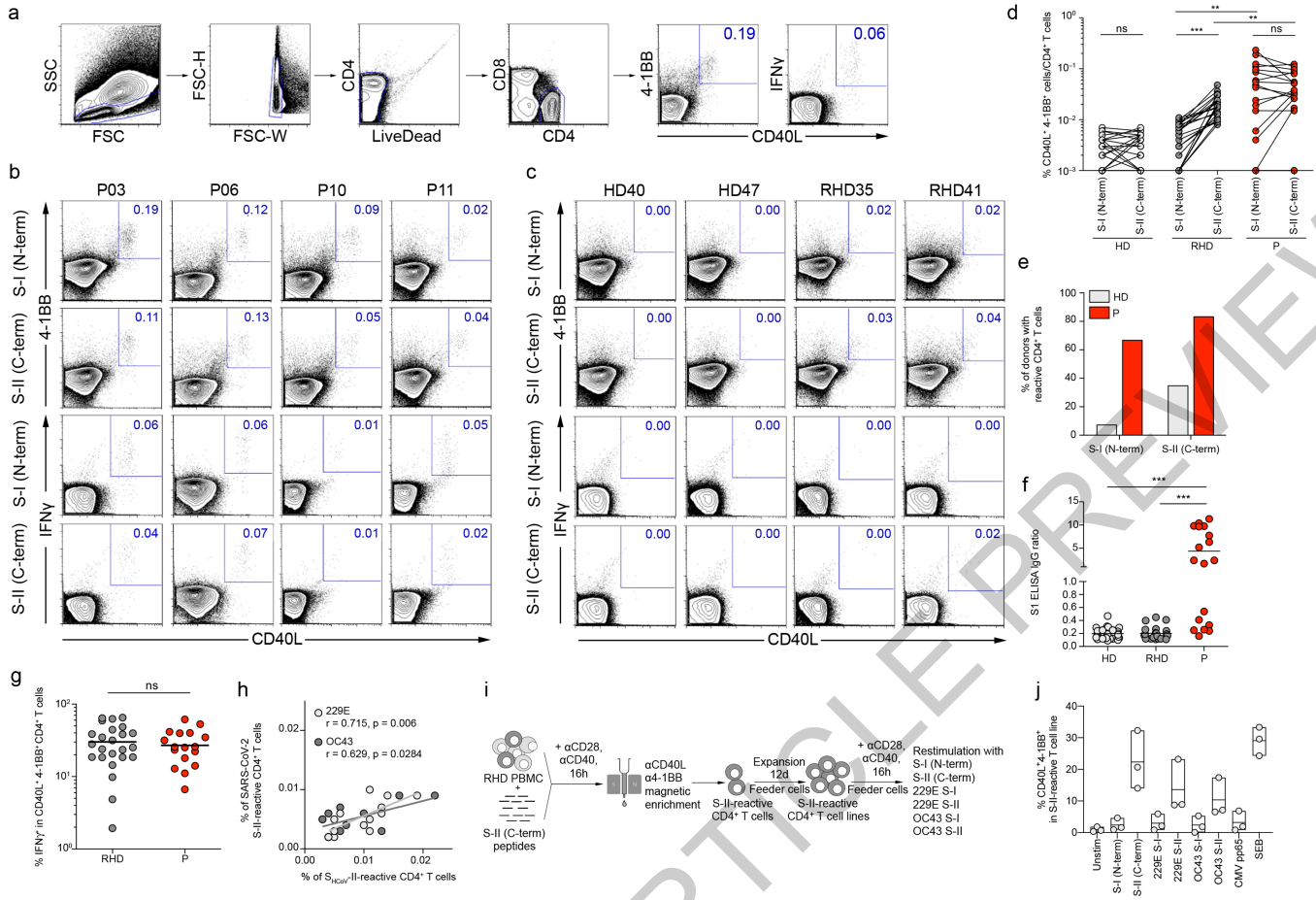

Fig. 2 | SARS-CoV-2 spike glycoprotein-reactive CD4⁺ T cells in COVID-19 patients and healthy donors. a, Gating strategy to detect SARS-CoV-2 S-reactive CD4⁺ T cells after 16 hours *in vitro* stimulation with PepMix™ SARS-CoV-2 spike glycoprotein peptide pool 1 (S-I (N-term)) and 2 (S-II (C-term)). Representative data of one COVID-19 patient is depicted. **b, c**, Representative plots displaying CD40L and 4-1BB as well as CD40L and IFN-γ expression on CD4⁺ T cells of COVID-19 patients (P), healthy donors (HD) and reactive healthy donors (RHD) after 16 hours *in vitro* stimulation with S-I (N-term) or S-II (C-term). Numbers are percent of double-positive cells from total CD4⁺ T cells. **d**, Comparison of S-I (N-term)- or S-II (C-term)-reactive CD40L⁺4-1BB⁺ CD4⁺ T cell frequencies of HD (n=44), RHD (*n*=24) and P (*n*=18). *p*-values (from left to right and top to bottom): ns: 0.1632, ***: <0.0001, **: 0.0031, **: 0.0059, ns: 0.9766. **e**, Percent of individuals from P and HD, respectively, with S-I (N-term)- and S-II (C-term)-reactive CD4⁺ T cells, respectively. **f**, SARS-CoV-2 S1 serology of HD (*n*=44), RHD (*n*=24) and P (*n*=18). *p*-values: upper ***: <0.0001, lower ***: <0.0001. **g**, Comparison of frequencies of IFN-γ⁺ cells among CD40L⁺4-1BB⁺ CD4⁺ T cells in RHD (*n*=24) and P (*n*=18). **h**, Correlation between SARS-CoV-2 S-II and S_{HCoV}-II CD4⁺ T cell responses. Frequencies of CD40L⁺ 4-1BB⁺ CD4⁺ T cells after stimulation with S-II peptide pools of SARS-CoV-2 (y-axis) and S-II peptide pools of HCoVs (x-axis) 229E (lightgrey, *n*=12) and OC43 (darkgrey, *n*=9) from RHD are shown. **i**, Schematic summary of SARS-CoV-2 S-II-reactive CD4⁺ T cell lines generation. **j**, Enriched and expanded SARS-CoV-2 S-II-reactive CD4⁺ T cells were re-stimulated with the indicated S-I and S-II peptide pools of SARS-CoV-2 and the two HCoV strains. Statistics: **d,f,g**, * p<0.05, ** p<0.01, *** p<0.001 as calculated by two-tailed Mann-Whitney U test; **i**, Correlation coefficient *r* was calculated by bivariate Pearson correlation and the related *p* value based on t-distribution.

ACCELERATED ARTICLE PREVIEW

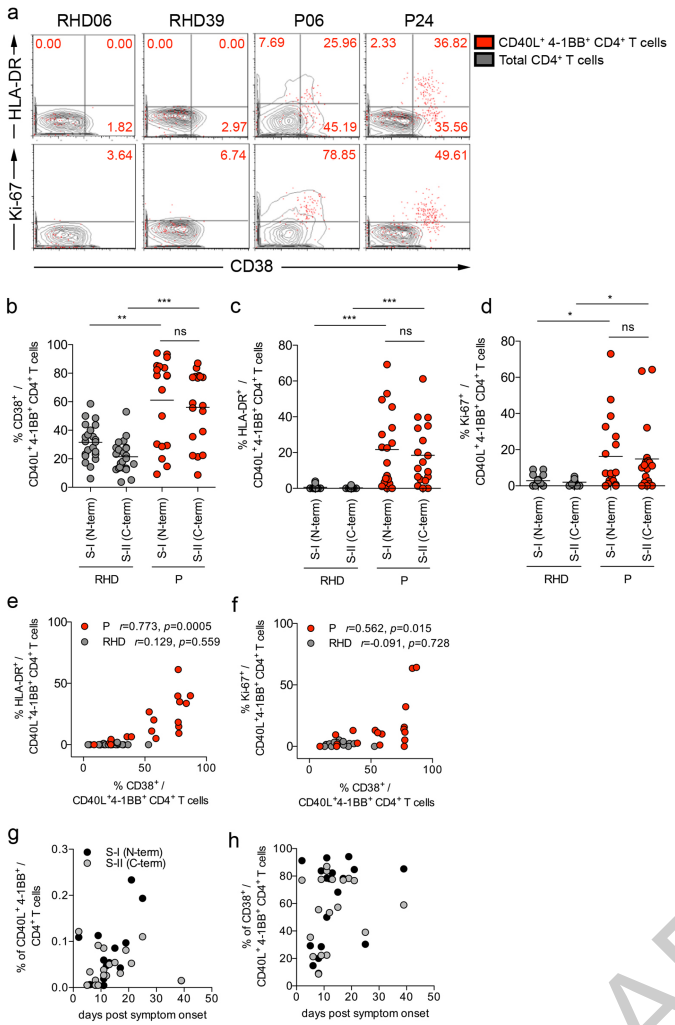

Fig. 3 | CD38, HLA-DR and Ki-67 expression of SARS-CoV-2 S-I- and S-II-reactive CD4$^+$ T cells discriminates SARS-CoV-2 patients from reactive healthy donors. a, Representative examples of HLA-DR and Ki-67 expression plotted against CD38 expression on S-II-reactive CD4$^+$ T cells (red dots) compared to total CD4$^+$ T cells (grey contours) in reactive healthy donors (RHD) and COVID-19 patients (P). **b-d**, Comparison of frequencies of CD38$^+$, HLA-DR$^+$ and Ki67$^+$ cells among S-I (N-term)- and S-II (C-term)-reactive CD4$^+$ T cells in RHD (**b,c**, *n*=23; **d**, *n*=17) and P (*n*=18). * p<0.05, ** p<0.01, *** p<0.001 as calculated by two-tailed Mann-Whitney U test. *p*-values (from left to right): b) **: 0.0060, ***: <0.0001, ns: 0.2482; c) ***: <0.0001, ***: <0.0001, ns: 0.8618; d) *: 0.0405, *: 0.0102, ns: 1.00. **e, f**, Co-expression of HLA-DR or Ki-67 and CD38 among S-II-reactive CD4$^+$ T cells from RHD (**e**, *n*=23; **f**, *n*=17) and P (*n*=18). **g, h**, Frequencies of S-I- and S-II-reactive CD40L$^+$4-1BB$^+$ CD4$^+$ T cells (g) or CD38$^+$ among S-II-reactive CD4$^+$ T cells (h) of P (*n*=18) plotted against days post symptom onset. Statistics: **b-d**, * p<0.05, ** p<0.01, *** p<0.001 as calculated by two-tailed Mann-Whitney U test; **e,f**, Correlation coefficient *r* was calculated by bivariate Pearson correlation and the related *p* value based on t-distribution.

ACCELERATED ARTICLE PREVIEW

Table 1 | Baseline characteristics of COVID-19 patients and healthy donors

Cohort	m:f	Age Avg (range)	severity	ICU (y/n)	Sampling day Avg (range)
COVID-19 patients	72 : 28%	52.6 (21-81 yrs)	mild 38.9% severe 27.8% critical 33.3%	n 44.4% y 55.6%	14.9 (2-39)
Healthy donors	31 : 59%	41.9 (20-64 yrs)	-	-	-

*Day after onset of symptoms, Avg: average, m: male, f: female, ICU: intensive care unit, y: yes, n: no.

ACCELERATED ARTICLE PREVIEW

Methods

Study subjects

The study was approved by the Institutional Review board of the Charité (EA2/066/20). After providing written informed consent, 68 healthy donors (HD, Extended Data Table 3, Table 2) and 18 and 7 additional COVID-19 patients (Table 1 and Extended Data Table 2 and 4) were included in the study. COVID-19 patients who tested positive for SARS-CoV-2 RNA in nasopharyngeal swabs were recruited at Charité Campus Virchow-Klinikum, Berlin, between March 1st and April, 2nd 2020. All COVID-19 patients were enrolled in the Berlin prospective observation COVID-19 study (PA-COVID-19)[36]. Disease severity was grouped based on requirement for supplemental oxygen or ventilation (mild; hospitalized, no supplemental oxygen, severe: hospitalized, supplemental oxygen (including High-flow), critical: hospitalized, invasive ventilation). For intracellular cytokine and memory T cell stainings, 7 additional COVID-19 patients (Extended Data Table 4) were enrolled at later time points and 5 RHD were re-recruited. To retrospectively validate SARS-CoV-2 seronegativity, all HD were re-invited between 4th and 7th May 2020 for re-assessment of anti-S1 IgG titers. 65 of 68 could be re-recruited and all were seronegative for SARS-CoV-2 (Extended Data Fig. 4).

Serology

Anti-SARS-CoV-2 IgG ELISA was performed using a commercial kit (EUROIMMUN) as described and validated before[37]. Recombinant immunofluorescence assays (rIFA) to determine IgG titers against HCoV were performed by using VeroB4 cells expressing cloned recombinant coronavirus spike proteins from HCoV-229E, HCoV-NL63, HCoV-OC43, HCoV-HKU1 as described in Corman et al.[38].

Cell isolation and stimulation

Peripheral blood mononuclear cells (PBMC) were isolated from heparinized whole blood by gradient density centrifugation according to manufacturer's instructions (Leucosep tubes, Greiner; Biocoll, Bio&SELL). Stimulation was conducted with $5x10^6$ PBMC in RPMI 1640 medium (Gibco) supplemented with 10% heat inactivated AB serum (Pan Biotech), 100 U/ml penicillin (Biochrom), 0.1 mg/ml streptomycin (Biochrom) and PepMix™ SARS-CoV-2 spike glycoprotein (JPT) peptide pool 1 or 2 in the presence of 1 µg/ml purified anti-CD28 (clone CD28.2, BD Biosciences). The PepMix™ SARS-CoV-2 spike glycoprotein pool 1 covering the N-terminal amino acid (aa) residues 1-643 (abbreviated to "S-I" (N-term)) contained 158 15-mers overlapping by 11 aa. PepMix™ SARS-CoV-2 spike glycoprotein pool 2 covered the C-terminal aa residues 633-1273 (abbreviated to "S-II" (C-term)) containing 156 15-mers overlapping by 11 aa and one 17-mer at the C-terminus, i.e. 157 peptides in total. Both peptide pools were used at 1 µg/ml per peptide, respectively. Further details on the peptide pools and predicted MHC-II epitopes are given in Fig. 1, Extended Data Fig. 1 and Extended Data Table 1. Stimulation controls were performed with equal concentrations of DMSO in PBS (unstimulated) or 1.5 mg SEB/1.0 mg TSST1 (Sigma-Aldrich) and PepMix™ HCMVA (pp65) (>90%; CMVpp65) (JPT) in the presence of 1 µg/ml purified anti-CD28 (clone CD28.2, BD Biosciences) as positive controls, respectively. Incubation was performed at 37˚C, 5% CO_2 for 16 h with 10 µg/ml brefeldin A (Sigma-Aldrich) added after 2 h. Stimulation was stopped by incubation in 2 mM EDTA for 5 min. Stimulation with HCoV spike glycoprotein (S_{HCoV}) peptide pools was conducted under the described conditions above but with 1 µg/ml per peptide of the following peptide pools: PepMix™ HCoV-229E spike glycoprotein pool 1 or 2 or PepMix™ HCoV-OC43 spike glycoprotein pool 1 or 2 (all JPT).

Flow Cytometry

After stimulation, surface stainings were conducted for 15 min with the following fluorochrome conjugated antibodies titrated to their optimal concentrations: CD38-PE-Vio770 (clone REA671, Miltenyi, dilution: 1:400), CD69-APC-Cy7 (FN50, Biolegend, 1:100), HLAD-DR-VioGreen (REA805, Miltenyi, 1:50), CD4-BrilliantViolet605 (RPA-T4, Biolegend, 1:200), CD8-PerCP (SK1, Biolegend, 1:100) with 1 mg/ml Beriglobin (CSL Behring) added prior to the staining. For exclusion of dead cells, Zombie Yellow fixable viability staining (Biolegend) was added for the last 10 min of incubation. Fixation and permeabilization were performed with eBioscience™ FoxP3 fixation and PermBuffer (Invitrogen) according to the manufacturer's protocol and intracellular staining carried out for 30 min in the dark at room temperature with Beriglobin added prior to staining with 4-1BB(CD137)-PE (clone 4B4-1, BD, 1:10), CD40L(CD154)-APC (5C8, Miltenyi, 1:40), IFNγ-AlexaFluor700 (B27, BD, 1:50), TNFα-PacificBlue (MAb11, Biolegend, 1:100) and Ki-67-AlexaFluor488 (B56, BD, 1:100). To assess naive/memory T cell phenotypes and cytokine expression, the following antibodies were used: surface staining was performed with CD3-V500 (SP34-2, BD, 1:50), CD8-PerCP (SK1, Biolegend, 1:100), CD4-BrilliantViolet605 (RPA-T4, Biolegend, 1:200), CCR7-AlexaFluor488 (G043H7, Biolegend, 1:150), CD45RA-PE-Cy7 (HI100, Biolegend, 1:200). IFNγ-AlexaFluor700 (B27, BD, 1:100), CD40L(CD154)-BrilliantViolet421 (24-31, Biolegend, 1:200), IL-2-APC (5344.111, BD, 1:200), 4-1BB(CD137)-PE (4B4-1, BD, 1:10) and IL-17A-APC-Cy7 (BL168, Biolegend, 1:20) were utilized for intracellular staining after fixation and permeabilization using BD FACSLysing Buffer and BD Perm2 Buffer, according to manufacturer's instructions. Samples were measured on a MACSQuant® Analyzer 16 using MACSQuantify software (v2.13). Instrument performance was monitored daily with Rainbow Calibration Particles (BD).

Cell enrichment, expansion, and restimulation

S-II-reactive T cells were enriched by magnetic cell sorting (MACS) from PBMC stimulated with PepMix™ SARS-CoV-2 spike glycoprotein peptide pool 2 (JPT) in the presence of 1 µg/ml purified anti-CD28 (clone CD28.2, BD Biosciences) and 1 µg/ml a-CD40 (clone 5C3, Biolegend). Following stimulation for 16 h, cells were stained with CD40L-APC and 4-1BB-PE and firstly enriched with anti-APC MultiSort MicroBeads (Miltenyi) according to manufacturer's instructions. After the release of anti-APC-MicroBeads, a second enrichment was performed with anti-PE MicroBeads (Miltenyi). Purity was checked each time to >80% of alive cells. APC feeder cells were generated by CD3 MicroBead (Miltenyi) depletion of the CD40L-APC-negative fraction and subsequent inactivation by irradiation at 50Gy. The irradiated feeder cells were co-cultured with the enriched $4\text{-}1BB^+CD40L^+$ T cells at a ratio of 1:1 in RPMI 1640 medium (Gibco) supplemented with 10% heat inactivated AB serum (Pan Biotech), 100 U/ml penicillin (Biochrom), 0.1 mg/ml streptomycin (Biochrom) in the presence of 10 ng/ml IL-7 and IL-15, respectively (both Miltenyi) for 12 days followed by 2 day cytokine starvation prior to restimulation. Restimulation was conducted with the described conditions above and additionally with 1 µg/ml per peptide of the following peptide pools: PepMix™ HCoV-229E spike glycoprotein pool 1 or 2 or PepMix™ HCoV-OC43 spike glycoprotein pool 1 or 2 (all JPT).

Data analysis and statistics

Sequence alignments have been performed using R (v3.6.1) including package ClustalX[39] and using the Needlemann-Wunsch algorithm[40]. Flow cytometry data were analyzed with FlowJo 9.9.6 (FlowJo LLC). Microsoft Excel (v14.1.0) and Prism 5 and 8 (GraphPad Inc.) was used for plotting and statistical analysis. In stimulation experiments, frequencies of activated $CD4^+$ T cells were background-subtracted, with the frequency in the unstimulated control sample representing the background. Non-parametric testing was used to compare cell frequencies and antibody titers between groups (two-tailed Mann-Whitney U test). *n* indicates the number of donors.

Reporting summary

Further information on research design is available in the Nature Research Reporting Summary linked to this paper.

ACCELERATED ARTICLE PREVIEW

Data availability

All flow cytometry data are made available in the FlowRepository.org (experiment ID: FR-FCM-Z2K3). An additional Supplementary Figure displaying the individual gating strategy for all donors is available in the online version of the paper.

31. Lidwell, O. M. & Williams, R. E. The epidemiology of the common cold. *I. J. Hyg. (Lond)*. **59**, 309–319 (1961).
32. Gaunt, E. R., Hardie, A., Claas, E. C. J., Simmonds, P. & Templeton, K. E. Epidemiology and clinical presentations of the four human coronaviruses 229E, HKU1, NL63, and OC43 detected over 3 years using a novel multiplex real-time PCR method. *J. Clin. Microbiol*. **48**, 2940–2947 (2010).
33. Callow, K. A., Parry, H. F., Sergeant, M. & Tyrrell, D. A. The time course of the immune response to experimental coronavirus infection of man. *Epidemiol. Infect.* **105**, 435–446 (1990).
34. Channappanavar, R., Fett, C., Zhao, J., Meyerholz, D. K. & Perlman, S. Virus-Specific Memory CD8 T Cells Provide Substantial Protection from Lethal Severe Acute Respiratory Syndrome Coronavirus Infection. *J. Virol*. **88**, 11034–11044 (2014).
35. Wang, B. *et al*. Identification of an HLA-A*0201-restricted CD8+ T-cell epitope SSp-1 of SARS-CoV spike protein. *Blood* **104**, 200–206 (2004).
36. Kurth, F. *et al*. Studying the pathophysiology of coronavirus disease 2019 - a protocol for the Berlin prospective COVID-19 patient cohort (Pa- COVID-19). *medRxiv* https://do, (2020).
37. Okba, N. M. A. *et al*. Severe Acute Respiratory Syndrome Coronavirus 2–Specific Antibody Responses in Coronavirus Disease 2019 Patients. *Emerg. Infect. Dis. J*. **26**, 2020.03.18.20038059 (2020).
38. Corman, V. M. *et al*. Assays for laboratory confirmation of novel human coronavirus (HCOV-EMC) infections. *Eurosurveillance* (2012). https://doi.org/10.2807/ese.17.49.20334-en
39. Larkin, M. A. *et al*. Clustal W and Clustal X version 2.0. *Bioinformatics* (2007). https://doi.org/10.1093/bioinformatics/btm404
40. Needleman, S. B. & Wunsch, C. D. A general method applicable to the search for similarities in the amino acid sequence of two proteins. *J. Mol. Biol*. (1970). https://doi.org/10.1016/0022-2836(70)90057-4

Acknowledgements We thank Ulf Klein (Leeds, UK) und Hans-Peter Herzel (Berlin) for critical discussion. We thank S. O. and J. S. for discussions and support. We thank Toralf Kaiser and Jenny Kirsch from the Flow Cytometry Core Facility (FCCF) of the DRFZ for expert technical help. We thank Bernd Timmerman from the Sequencing Core Facility of the Max Planck Institute for Molecular Genetics for discussion. This work was supported by the German Research Foundation (KFO339 to JB and FF, SFB-TR84 projects A4, B6 to SH, B8 to MM, C6 to MW, C8, C10 to LES, C9 to MW, NS) and by the German Federal Ministry of Education and Research (BMBF-RAPID to SH, CD, and CAPSyS to MW, NS). This work was additionally funded by the Federal Ministery of Health through a resolution of the German Bundestag to AT, JB, LH and MD.

Author contributions JB, LL and MF planned and performed experiments and analyzed the data. DW, PG, JR, MD, BK, FF, EB, MM, LH performed experiments. FK, AH, SH, KB, ID, MAM, SV, MW, NS, CD, LES managed initial patient contacts, designed and supervised clinical management and clinical data. MAM and VMC planned and performed experiments and analyzed the data. JS and SM established high-throughput analysis. RL designed experiments. FK, UR and HW established new reagents. GCT and AT designed and supervised the study. CGT, LES and AT wrote the manuscript.

Competing interests FK, UR and HW are employed at JPT Peptide Technologies, who have provided peptide pools for this work. FK also part-owns and is inventor on a patent describing the use of overlapping peptide pools for the stimulation of T cells. Until this patent expires, he will receive royalties on JPT PepMix sales. JS and SM are employed at Miltenyi Biotec, who provided reagents and devices for this study. All other authors declare no competing interests.

Additional information

Supplementary information is available for this paper at https://doi.org/10.1038/s41586-020-2598-9.

Correspondence and requests for materials should be addressed to C.G.-T., L.E.S. or A.T.

Peer review information *Nature* thanks Akiko Iwasaki and the other, anonymous, reviewer(s) for their contribution to the peer review of this work. Peer reviewer reports are available.

Reprints and permissions information is available at http://www.nature.com/reprints.

ACCELERATED ARTICLE PREVIEW

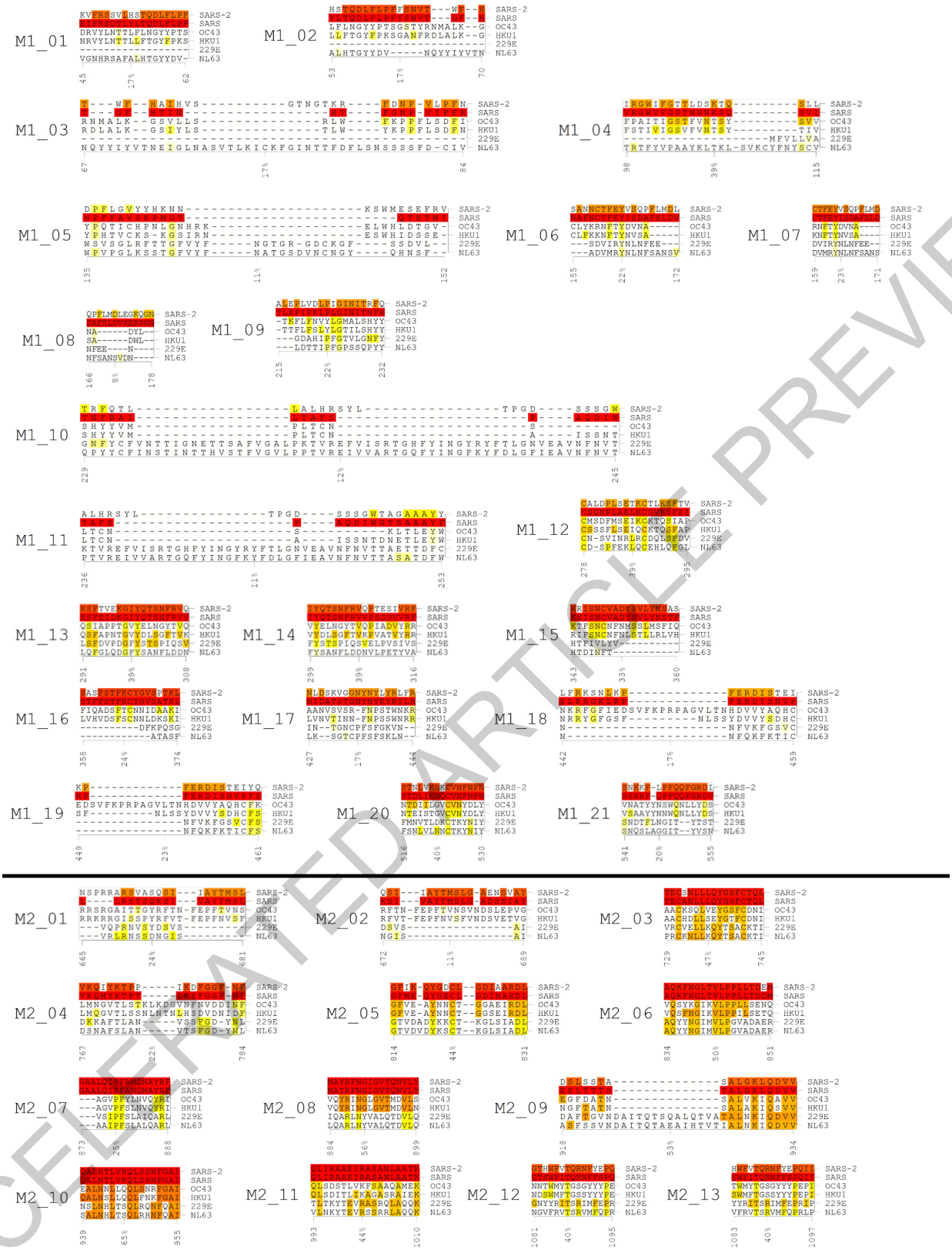

Extended Data Fig. 1 | Homology of reported MHC-II epitopes from Extended Data Table 1 in the spike glycoprotein of SARS-CoV to SARS-CoV-2 and endemic coronavirus strains. Shown is for each epitope the respective section from a global sequence alignment between the 6 indicated coronaviruses. Identical residues are color-coded from white (no identity) to red (100% identity).

ACCELERATED ARTICLE PREVIEW

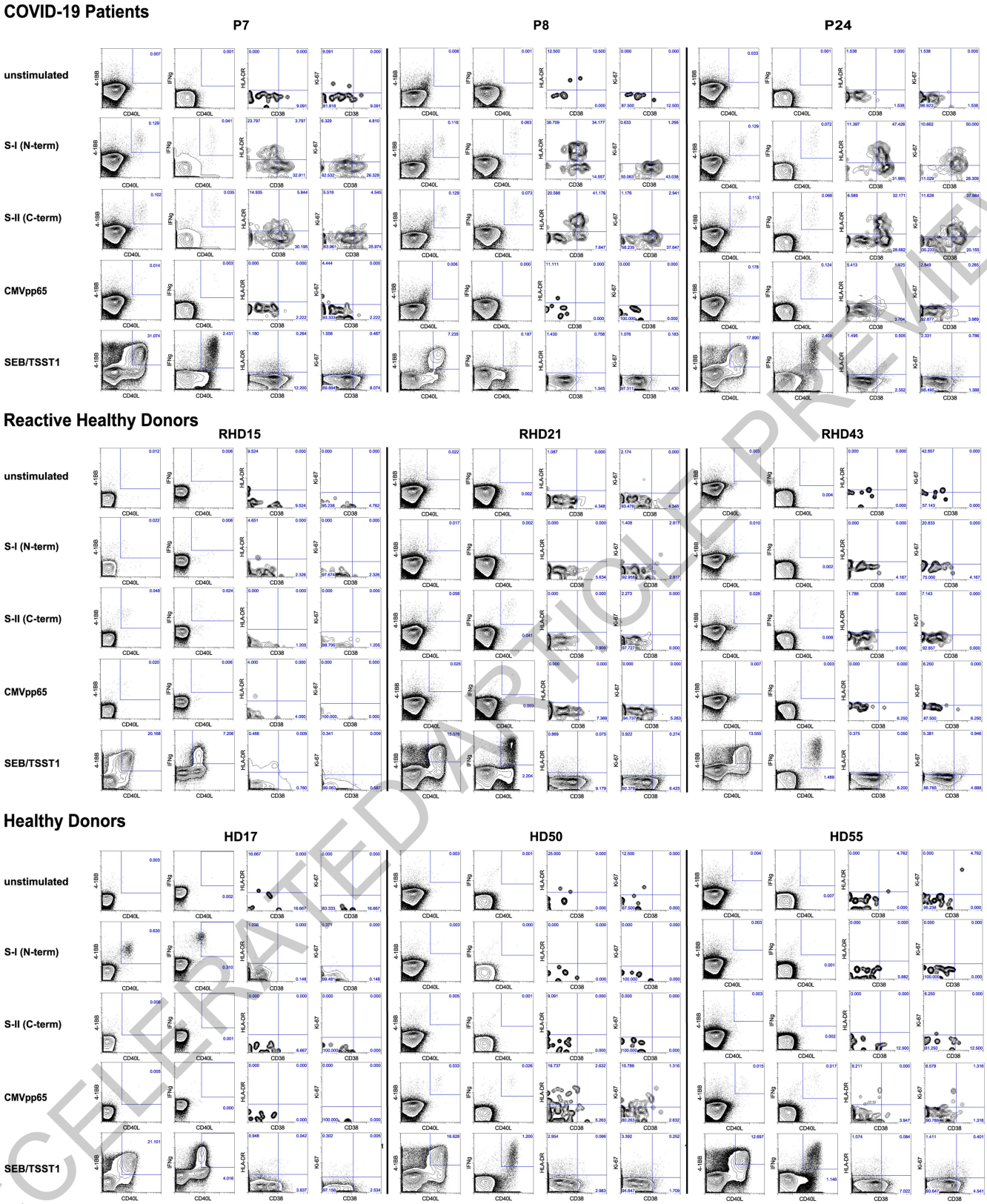

Extended Data Fig. 2 | Overview of the analyses gates and dot plots from COVID-19 patients, reactive healthy donors (RHD) and healthy donors (HD) to determine the frequencies of S-I- and S-II-reactive CD4$^+$ T cells and the ratios of CD38$^+$, HLA-DR$^+$ and Ki-67$^+$ cells among them.

ACCELERATED ARTICLE PREVIEW

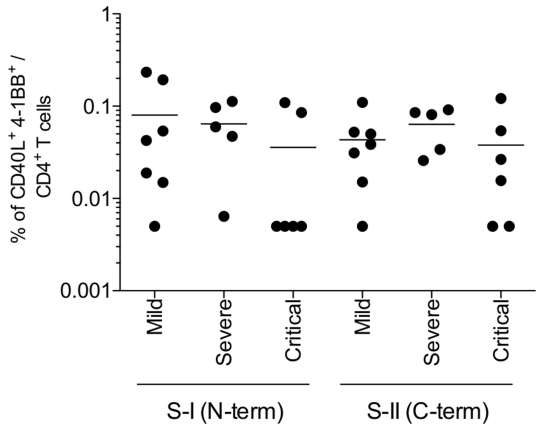

Extended Data Fig. 3 | Most S-I- and S-II-non-reactive COVID-19 patients had a critical disease stage. Frequencies of S-I- and S-II-reactive $CD4^+$ T cells in COVID-19 patients are grouped according to disease severity in mild (*n*=7), severe (*n*=5) and critical (*n*=6).

ACCELERATED ARTICLE PREVIEW

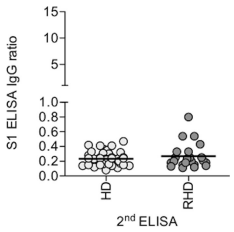

Extended Data Fig. 4 | Repeated serology of HD confirms unexposed status of HD and RHD. SARS-CoV-2 S1 serology of HD (n=43) and RHD (n=22) more than 28 days after initial sampling. Anti-spike glycoprotein subunit 1 (S1) IgG titers are expressed as ratio normalized to calibrator well.

ACCELERATED ARTICLE PREVIEW

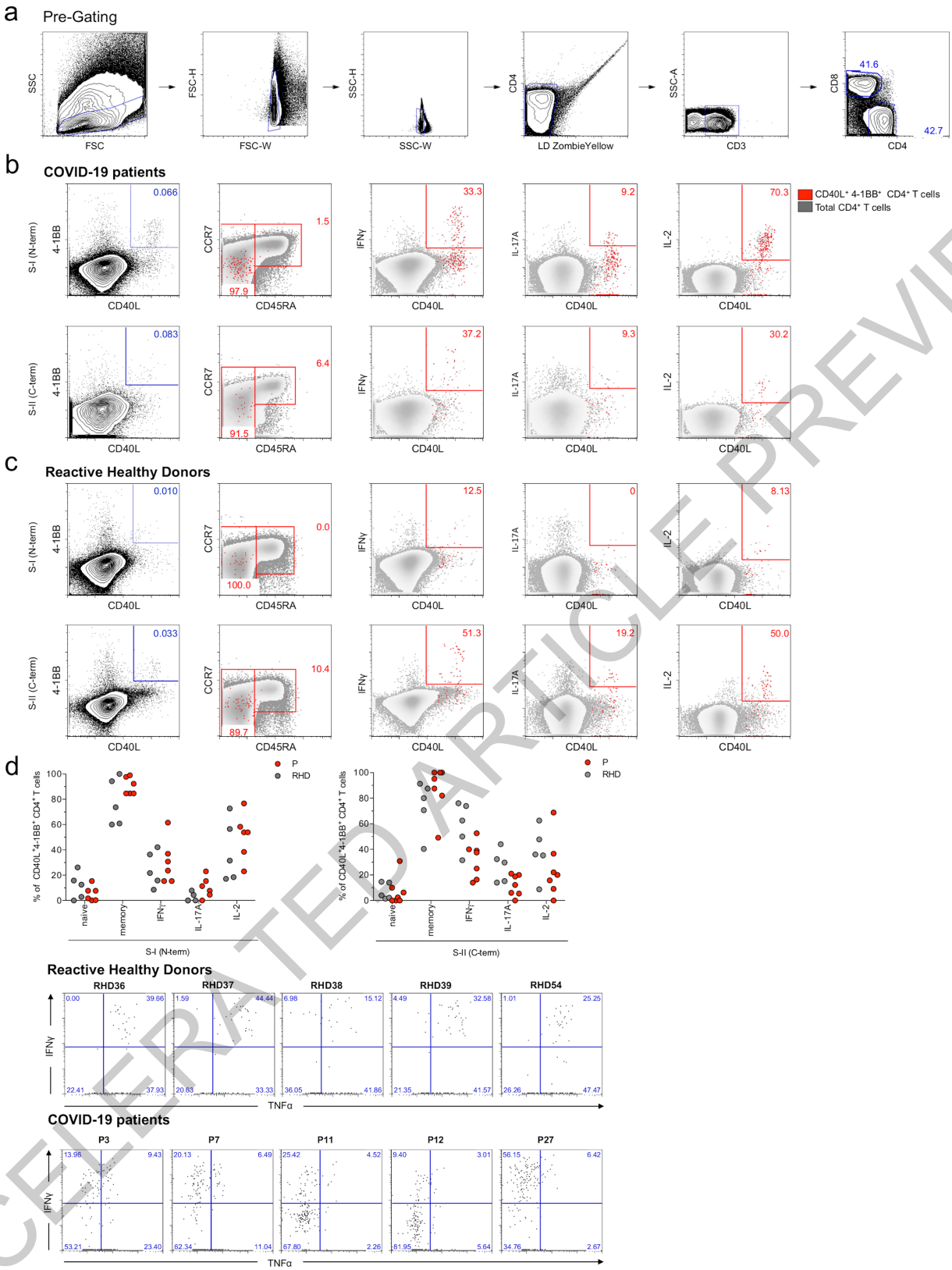

Extended Data Fig. 5 | Cytokine and differentiation marker expression of S-I- and S-II-reactive CD40L$^+$4-1BB$^+$CD4$^+$ T cells from COVID-19 patients and RHD. a, Gating scheme of one representative donor to select CD3$^+$CD4$^+$ T cells and exclude dead cells and doublets. **b, c**, Determination of the differentiation marker and cytokine profile of S-I-/S-II-reactive CD4$^+$ T cells exemplarily shown for one COVID-19 patient (P) and one reactive healthy donor (RHD) after S-I and S-II peptide pool stimulation, respectively. SARS-CoV-2 S-reactive CD4$^+$ T cells were defined by CD40L and 4-1BB expression post stimulation and are displayed as red dots in the subsequent dotplots. Numbers are the frequencies of cytokine expressing cells of S-I-/S-II-reactive CD4$^+$ T cells and distribution between naïve (CCR7$^+$CD45RA$^+$) and memory (CCR7$^{+/-}$CD45RA$^-$) phenotype of S-I-/S-II-reactive CD4$^+$ T cells, respectively. **d**, Diagrams summarizing the cytokine and differentiation marker distribution frequencies of S-I- and S-II-reactive CD4$^+$ T cells from seven patients and five RHD. **e**, Expression of TNFα and IFNγ in S-II-reactive CD4$^+$ T cells in P and RHD. Five representative plots of TNFα versus IFNγ expression in CD40L$^+$4-1BB$^+$ CD4$^+$ T cells in reactive healthy donors (RHD) and COVID-19 patients (P), gating strategy as shown in Fig. 2.

ACCELERATED ARTICLE PREVIEW

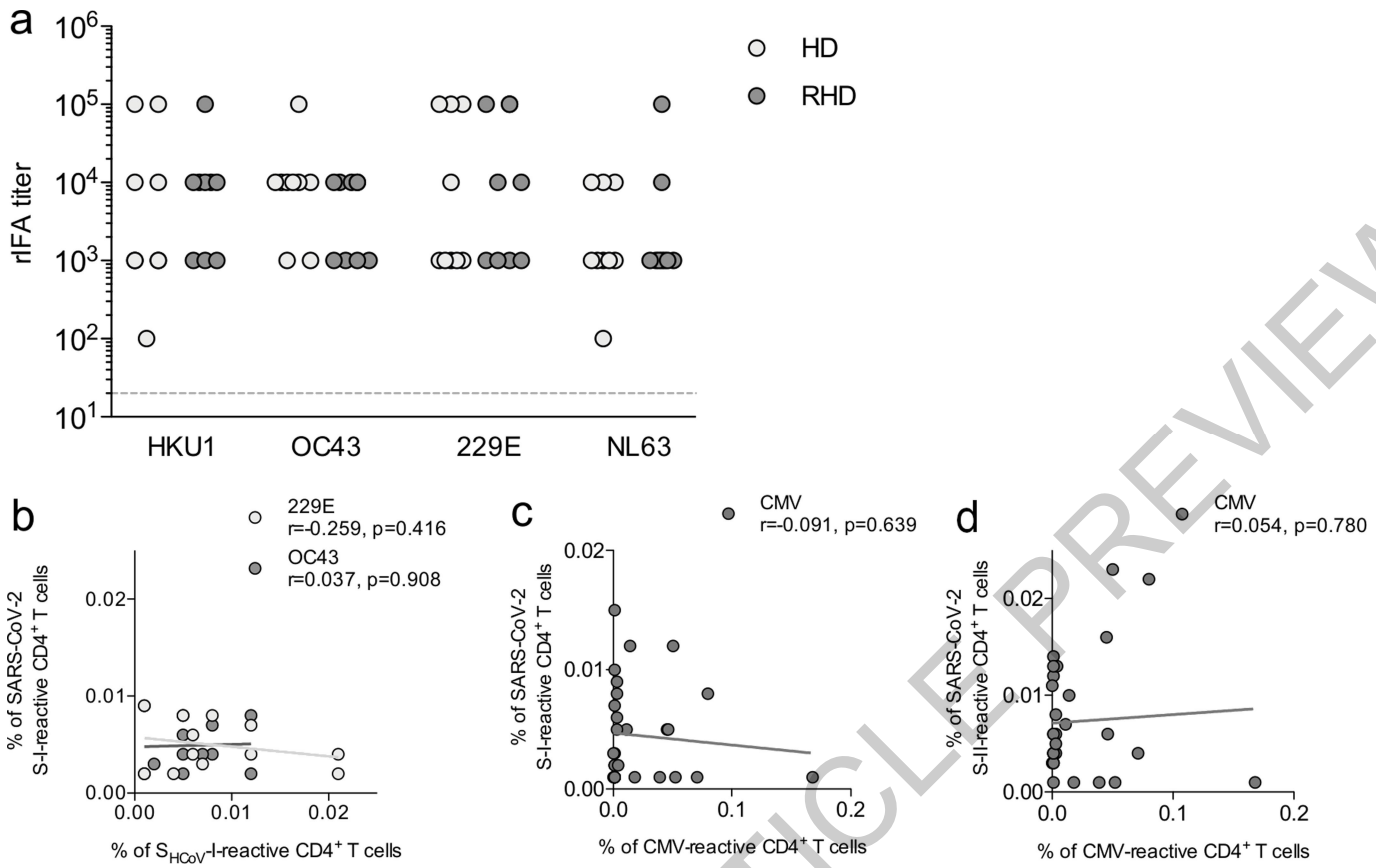

Extended Data Fig. 6 | HCoV-specific IgG antibody titres in HD and RHD and specificity of SARS-CoV-2-reactive T cells in HD. a) IgG antibody titers against endemic coronavirus strains (HCoV). VeroB4 cells expressing recombinant spike (S) proteins of HCoV-HKU1, HCoV-OC43, HCoV-229E and HCoV-NL63, respectively, were used in a recombinant immunofluorescence assay (rIFA) as outlined in Corman et al. 2012. Titers above 1:20 dilution were considered positive (indicated by dashed line). HD: healthy donor (n=9); RHD: reactive healthy donor (n=9). **b-d**, Frequencies of SARS-CoV-2 S-I-reactive CD4$^+$ T cells in healthy donors do not correlate with frequencies of S_{HCoV}-I-reactive or CMV-reactive CD4$^+$ T cells and frequencies of SARS-CoV-2 S-II-reactive CD4$^+$ T cells in healthy donors do not correlate with frequencies of CMV-reactive CD4$^+$ T cells **b**, Scatter plot of S_{HCoV}-I-reactive CD4$^+$ T cell (for 229E (n=12) and OC43 (n=9)), respectively) and SARS-CoV-2 S-I-reactive CD4$^+$ T cell frequencies. **c**, Scatter plot of SARS-CoV-2 S-I-reactive CD4$^+$ T cell and CMV-reactive CD4$^+$ T cell frequencies (n=21). **d**, Scatter plot of SARS-CoV-2 S-II-reactive CD4$^+$ T cell and CMV-reactive CD4$^+$ T cell frequencies (n=21). Statistics: **c - d**, Correlation coefficient r was calculated by Pearson correlation and the related p value based on t-distribution.

ACCELERATED ARTICLE PREVIEW

Extended Data Table 1 | Reported MHC-II epitopes in the spike glycoprotein of SARS-CoV with identity calculation for SARS-CoV-2 and the HCoVs NL63, 229E, HKU1, and OC43 (maximum identity)

ID	PepMix™	Sequence	Maximum identity common cold viruses (%)	Identity SARS-CoV-2	Start position SARS	Stop position SARS	Reference
M1_1	1	EIFRSDTLYLTQDLFLPF	16,7	66,7	45	62	14
M1_2	1	YLTQDLFLPFYSNVTGFH	16,7	77,8	53	70	14
M1_3	1	TGFHTINHTFGNPVIPFK	16,7	55,6	67	84	14
M1_4	1	VRGWVFGSTMNNKSQSVI	38,9	50	98	115	14
M1_5	1	NPFFAVSKPMGTQTHTMI	11,1	16,7	135	152	14
M1_6	1	NAFNCTFEYISDAFSLDV	22,2	55,6	155	172	14
M1_7	1	CTFEYISDAFSLD	23,1	61,5	159	171	14
M1_8	1	DAFSLDVSEKSGN	7,7	38,5	166	178	14
M1_9	1	TLKPIFKLPLGINITNFR	22,2	55,6	215	232	14
M1_10	1	TNFRAILTAFSPAQDIW	11,8	23,5	229	245	14
M1_11	1	TAFSPAQDIWGTSAAAYF	11,1	27,8	236	253	14
M1_12	1	CSQNPLAELKCSVKSFEI	38,9	50	278	295	14
M1_13	1	KSFEIDKGIYQTSNFRVV	38,9	77,8	291	308	14
M1_14	1	IYQTSNFRVVPSGDVVRF	38,9	72,2	299	316	14
M1_15	1	KKISNCVADYSVLYNSTF	33,3	83,3	343	360	14
M1_16	1	STFFSTFKCYGVSATKL	23,5	82,4	358	374	13;14
M1_17	1	NIDATSTGNYNYKYRYLR	16,7	55,6	427	444	13
M1_18	1	YLRHGKLRPFERDISNVP	16,7	50	442	459	14
M1_19	1	RPFERDISNVPFS	23,1	53,8	449	461	14
M1_20	1	STDLIKNQCVNFNFN	40	80	516	530	15
M1_21	1	SSKRFQPFQQFGRDV	20	73,3	541	555	15
		Mean Identity PepMix™ 1	23,2	57,5			
M2_1	2	LLRSTSQKSIVAYTMSL	23,5	58,8	665	681	14
M2_2	2	KSIVAYTMSLGADSSIAY	11,1	72,2	672	689	14
M2_3	2	TECANLLLQYGSFCTQL	47,1	94,1	729	745	13
M2_4	2	VKQMYKTPTLKYFGGFNF	22,2	77,8	767	784	14
M2_5	2	GFMKQYGECLGDINARDL	44,4	83,3	814	831	14
M2_6	2	AQKFNGLTVLPPLLTDDM	50	94,4	834	851	14
M2_7	2	GAALQIPFAMQMAYRF	25	100	873	888	14
M2_8	2	MAYRFNGIGVTQNVLY	56,2	100	884	899	14
M2_9	2	ESLTTTSTALGKLQDVV	52,9	70,6	918	934	14
M2_10	2	QALNTLVKQLSSNFGAI	64,7	100	939	955	14
M2_11	2	QLIRAAEIRASANLAATK	44,4	100	993	1010	14
M2_12	2	GTSWFITQRNFFSPQ	40	73,3	1081	1095	15
M2_13	2	SWFITQRNFFSPQII	40	73,3	1083	1097	14
		Mean Identity PepMix™ 2	40,1	84,4			

ACCELERATED ARTICLE PREVIEW

Extended Data Table 2 | Baseline characteristics of hospitalized COVID-19 patients

COVID-19 patients						
ID	**Severity**	**Gender**	**Age**	**Chief complaints at admission**	**ICU (y/n)**	**Sampling (day)***
P01	mild	m	21	Fever, dry cough, malaise	n	39
P03	mild	m	45	Fever, dry cough, runny nose	n	25
P10	mild	f	50	Fever, dry cough, myalgia, cephalgia, diarrhea	n	17
P18	mild	f	60	Fever, myalgia, cephalgia, runny nose	n	21
P19	mild	m	52	Dry cough, cephalgia, arthralgia, nausea	n	11
P23	mild	f	44	Fever	n	5
P27	mild	f	41	Fever, dry cough	n	13
P06	severe	m	24	Fever, dyspnea, malaise	y	11
P07	severe	m	33	Fever, dry cough, dyspnea, myalgia	n	5
P11	severe	m	61	Fever, dry cough, dyspnea, sore throat	y	12
P16	severe	m	74	Fever, dry cough, dyspnea, malaise	y	12
P24	severe	m	64	Fever, dry cough, dyspnea	y	19
P08	critical	m	63	Fever, dyspnea	y	2
P12	critical	m	75	Fever, dyspnea, malaise	y	8
P14	critical	m	81	Fever, dyspnea	y	8
P15	critical	m	54	Dry cough, dyspnea	y	6
P20	critical	f	53	Dry cough, dyspnea	y	11
P21	critical	m	52	Dry cough, dyspnea	y	9

*Day after onset of symptoms, m: male, f: female, ICU: intensive care unit, y: yes, n: no.

ACCELERATED ARTICLE PREVIEW

Extended Data Table 3 | Baseline characteristics of healthy donors

Healthy donors							
ID	Gender	Age	Health status	ID	Gender	Age	Health status
HD01	m	56		HD38	f	30	Allergies
HD02	m	48		HD39	f	41	
HD03	m	37		HD40	f	53	
HD04	f	40		HD41	m	42	
HD05	f	22		HD42	f	55	
HD06	m	30		HD43	m	25	
HD07	m	25		HD44	f	53	Hashimoto Thyreoiditis
HD08	m	41		HD45	f	47	
HD09	m	37		HD46	f	31	
HD10	m	40		HD47	f	46	
HD11	f	28		HD48	m	31	
HD12	f	43		HD49	m	44	
HD13	m	44	Allergies	HD50	f	60	
HD14	f	27		HD51	f	43	
HD15	m	32		HD52	f	20	
HD16	m	24		HD53	f	46	
HD17	m	42		HD54	m	24	
HD18	m	40		HD55	f	40	
HD19	f	26		HD56	f	40	
HD20	f	33		HD57	f	50	
HD21	m	30		HD58	f	30	
HD22	m	29		HD59	f	46	Allergies
HD23	f	38		HD60	f	31	
HD24	m	25		HD61	f	52	
HD25	m	48		HD62	f	53	Adenoma (surgically removed)
HD26	f	30		HD63	f	40	
HD27	m	64		HD64	f	27	
HD28	f	22		HD65	m	52	
HD29	f	40		HD66	f	42	
HD30	f	30		HD67	f	25	
HD34	f	55		HD68	m	38	
HD35	m	38	Thyroid dysfunction	HD70	f	22	
HD36	m	27		HD71	m	30	
HD37	f	26		HD72	f	64	

m: male; f: female.

ACCELERATED ARTICLE PREVIEW

Extended Data Table 4 | Baseline characteristics of 7 COVID-19 patients enrolled for cytokine staining

ID	Severity	Gender	Age	Chief complaints at admission	ICU (y/n)	Sampling (day)*
P153	mild	m	56	Dry cough, dyspnea, aeguisa	n	11
P158	mild	m	26	Fever, dry cough	n	10
P51	severe	m	79	Fever, dry cough, dyspnea	y	52
P131	severe	f	71	Malaise, rash	y	33
P157	severe	m	50	Fever, cough, malaise	y	23
P134	critical	m	27	Dyspnea	y	39
P142	critical	m	62	Fever cough, dyspnea	y	53

*Day after onset of symptoms, m: male, f: female, ICU: intensive care unit, y: yes, n: no.

ACCELERATED ARTICLE PREVIEW

nature research

Corresponding author(s): Andreas Thiel

Last updated by author(s): May 13, 2020

Reporting Summary

Nature Research wishes to improve the reproducibility of the work that we publish. This form provides structure for consistency and transparency in reporting. For further information on Nature Research policies, see Authors & Referees and the Editorial Policy Checklist.

Statistics

For all statistical analyses, confirm that the following items are present in the figure legend, table legend, main text, or Methods section.

n/a	Confirmed	
☐	☒	The exact sample size (*n*) for each experimental group/condition, given as a discrete number and unit of measurement
☐	☒	A statement on whether measurements were taken from distinct samples or whether the same sample was measured repeatedly
☐	☒	The statistical test(s) used AND whether they are one- or two-sided *Only common tests should be described solely by name; describe more complex techniques in the Methods section.*
☒	☐	A description of all covariates tested
☐	☒	A description of any assumptions or corrections, such as tests of normality and adjustment for multiple comparisons
☐	☒	A full description of the statistical parameters including central tendency (e.g. means) or other basic estimates (e.g. regression coefficient) AND variation (e.g. standard deviation) or associated estimates of uncertainty (e.g. confidence intervals)
☐	☒	For null hypothesis testing, the test statistic (e.g. *F*, *t*, *r*) with confidence intervals, effect sizes, degrees of freedom and *P* value noted *Give P values as exact values whenever suitable.*
☒	☐	For Bayesian analysis, information on the choice of priors and Markov chain Monte Carlo settings
☒	☐	For hierarchical and complex designs, identification of the appropriate level for tests and full reporting of outcomes
☐	☒	Estimates of effect sizes (e.g. Cohen's *d*, Pearson's *r*), indicating how they were calculated

Our web collection on statistics for biologists contains articles on many of the points above.

Software and code

Policy information about availability of computer code

Data collection	Miltenyi MACSquantify software v2.13 was used for flow cytometry data collection.
Data analysis	All the softwares and there version information are shown her. FlowJo (v9.9.6) was used for all FACS analyses. Microsoft Excel (v.14.1.0) was used to collect and arrange data and patient / donor information. GraphPad Prism (v5.0b and v8.4.2. (464)) was used to analyze data and create plots. Sequence alignments have been performed using R (v3.6.1) including package ClustalX (Larkin,M.A., Blackshields, G., Brown, N.P., Chenna, R., McGettigan, P.A., McWilliam, H., Valentin, F., Wallace, I.M., Wilm, A., Lopez, R., Thompson, J.D., Gibson, T.J., Higgins, D.G. (2007) Clustal W and Clustal X version 2.0. Bioinformatics, 23:2947-2948.) and using the Needlemann-Wunsch algorithm (Needleman S., Wunsch C. (1970) A general method applicable to the search for similarities in the amino acid sequence of two proteins. Journal of Molecular Biology, 48(3): 443-453).

For manuscripts utilizing custom algorithms or software that are central to the research but not yet described in published literature, software must be made available to editors/reviewers. We strongly encourage code deposition in a community repository (e.g. GitHub). See the Nature Research guidelines for submitting code & software for further information.

Data

Policy information about availability of data

All manuscripts must include a data availability statement. This statement should provide the following information, where applicable:

- Accession codes, unique identifiers, or web links for publicly available datasets
- A list of figures that have associated raw data
- A description of any restrictions on data availability

All flow cytometry data are made available in the FlowRepository.org (experiment ID: FR-FCM-Z2K3). An additional Supplementary Figure displaying the individual gating strategy for all donors is available in the online version of the paper.

Field-specific reporting

Please select the one below that is the best fit for your research. If you are not sure, read the appropriate sections before making your selection.

☒ Life sciences ☐ Behavioural & social sciences ☐ Ecological, evolutionary & environmental sciences

For a reference copy of the document with all sections, see nature.com/documents/nr-reporting-summary-flat.pdf

Life sciences study design

All studies must disclose on these points even when the disclosure is negative.

Sample size	No sample size calculation was performed. Within COVID-19 patients, 83% exhibited T cell reactivity to the Spike glycoprotein of SARS-CoV-2. Within the healthy donors recruited, 35% were identified as reactive healthy donors. With these proportions, the recruited numbers of subjects are sufficient.
Data exclusions	No data were excluded from the analyses.
Replication	We remeasured several donors (accompanied by anti-SARS-CoV-2 IgG antibody testing) at later timepoints and used another Spike glycoprotein peptide pool from Miltenyi to ensure reproducibility of T cell reactivity in SARS-CoV-2 naive donors.
Randomization	No randomization was performed since it was not applicable to the study.
Blinding	Blinding was not applicable to this study.

Reporting for specific materials, systems and methods

We require information from authors about some types of materials, experimental systems and methods used in many studies. Here, indicate whether each material, system or method listed is relevant to your study. If you are not sure if a list item applies to your research, read the appropriate section before selecting a response.

Materials & experimental systems

n/a	Involved in the study
☐	☒ Antibodies
☒	☐ Eukaryotic cell lines
☒	☐ Palaeontology
☒	☐ Animals and other organisms
☐	☒ Human research participants
☒	☐ Clinical data

Methods

n/a	Involved in the study
☒	☐ ChIP-seq
☐	☒ Flow cytometry
☒	☐ MRI-based neuroimaging

Antibodies

Antibodies used	CD69-APCCy7 BioLegend Cat# 310914, RRID:AB_314849 CD4-BV605 BioLegend Cat# 300556, RRID:AB_2564391 CD8-PerCp BioLegend Cat# 344708, RRID:AB_1967149 IFNg-AlexaFluor700 BioLegend Cat# 502520, RRID:AB_528921 TNFa-PB BioLegend Cat# 502920, RRID:AB_528965 CD38-PeVio770 Miltenyi Biotec Cat# 130-118-982, RRID:AB_2751601 HLADR-VG Miltenyi Biotec Cat# 130-111-795, RRID:AB_2652164 CD154(CD40L)-APC Miltenyi Biotec Cat# 130-113-603, RRID:AB_2726191 CD137(4-1BB)-PE BD Biosciences Cat# 555956, RRID:AB_396252 CD154(CD40L)-BV421 BioLegend Cat# 310824, RRID:AB_2562721 IL-2-APC BD Biosciences Cat# 341116, RRID:AB_400574 IL-17A-APCCy7 BioLegend Cat# 512320, RRID:AB_10613103 CCR7-AlexaFluor488 BioLegend Cat# 353206, RRID:AB_10916389 CD45RA-PeCy7 BioLegend Cat# 304126, RRID:AB_10708879 CD3-V500 BD Biosciences Cat# 560770, RRID:AB_1937322 Ki-67 AlexaFluor488 BD Biosciences Cat#558616, RRID:AB_647087 anti-CD28 BD Biosciences Cat#555725, RRID:AB_396068
Validation	All antibodies are established, well described and published elsewhere. Informations are accessible on the manufacturers websites under Catalogue or RRID numbers.

Human research participants

Policy information about studies involving human research participants

Population characteristics	The study included: - 18 COVID-19 patients (age mean 52.6, range: 21-81 yrs; gender: female ratio 27.8%; sampling day (post symptom onset): mean 14.9, range: 2-39 - 68 healthy donors (age mean 41.93, range: 20-64 yrs; gender: female ratio 59%) All healthy donors stated to be free of symptoms indicating an acute infection.
Recruitment	Patients were hospitalised in the Charité. The patients were selected based on disease severity to achieve a balanced representation of the three disease severity groups.
Ethics oversight	Institutional Review Board of the Charité.

Note that full information on the approval of the study protocol must also be provided in the manuscript.

Flow Cytometry

Plots

Confirm that:

☒ The axis labels state the marker and fluorochrome used (e.g. CD4-FITC).

☒ The axis scales are clearly visible. Include numbers along axes only for bottom left plot of group (a 'group' is an analysis of identical markers).

☒ All plots are contour plots with outliers or pseudocolor plots.

☒ A numerical value for number of cells or percentage (with statistics) is provided.

Methodology

Sample preparation	Peripheral blood mononuclear cells (PBMC) were isolated from heparinized whole blood by gradient density centrifugation according to manufacturer's instructions (Leucosep tubes, Greiner; Biocoll, Bio&SELL). Stimulation was conducted with 5x10e6 PBMC in RPMI 1640 medium (Gibco) supplemented with 10% heat inactivated AB serum (Pan Biotech), 100 U/ml penicillin (Biochrom), 0.1 mg/ml streptomycin (Biochrom), and PepMixTM SARS-CoV-2 in the presence of 1 µg/ml purified anti-CD28 (clone CD28.2, BD Biosciences). PepMixTM SARS-CoV-2 (Spike Glycoprotein) subpool 1 covering the N-terminal aa 1-643 (abbreviated to "S-I (N-term)") containing 158 15-mers overlapping by 11 and PepMixTM SARS-CoV-2 (Spike Glycoprotein) subpool 2 covering the C-terminal aa 633-1273 (abbreviated to "S-II (C-term)") (JPT) containing 156 15-mers overlapping by 11 and one 17-mer at C-terminus were used at 1 µg/ml per peptide, respectively. Stimulation controls were performed with equal concentrations of DMSO in PBS (unstimulated) or 1.5 mg SEB/1.0 mg TSST1 (Sigma-Aldrich) and PepMixTM CMV pp65 (Miltenyi) as positive controls, respectively. Incubation was performed at 37˚C, 5% CO2 for 14h with 10 µg/ml brefeldin A (Sigma- Aldrich) added after 2 h. Stimulation was stopped by incubation in 20 mM EDTA for 5 min and surface staining conducted for 15 min with the following fluorochrome conjugated antibodies titrated to their optimal concentrations: CD38-PE-Vio770 (clone REA671, Miltenyi), CD69-APC-Cy7 (FN50, Biolegend), HLAD-DR-VioGreen (REA805, Miltenyi), CD4-BrilliantViolet605 (RPA-T4, Biolegend), CD8-PerCP (SK1, Biolegend) with 1 mg/ml Beriglobin (CSL Behring) added prior to the staining. For exclusion of dead cells, Zombie Yellow fixable viability staining (Biolegend) was added for the last 10 min of incubation. Fixation and permeabilization were performed with eBioscienceTM FoxP3 fixation and PermBuffer (Invitrogen) according to the manufacturer's protocol and intracellular staining carried out for 30 min in the dark at room temperature with Beriglobin added prior to intracellular staining with 4-1BB-PE (clone 4B4-1, BD), CD40L-APC (5C8, Miltenyi) and Ki-67-AlexaFluor488 (B56, BD). For intracellular cytokine staining, we employed different antibodies. Surface staining was performed with CD3-V500 (SP34-2, BD), CD8-PerCP (SK1, Biolegend), CD4-BrilliantViolet605 (RPA-T4, Biolegend), CCR7-AlexaFluor488 (G043H7, Biolegend), CD45RA-PE-Cy7 (HI100, Biolegend). IFN-γ-AlexaFluor700, CD40L-BrilliantViolet421 (24-31, Biolegend), IL-2-APC (5344.111, BD), 4-1BB-PE (4B4-1, BD) and IL-17A-APC-Cy7 (BL168, Biolegend) were utilized for intracellular staining after fixation and permeabilization using BD FACSLysing Buffer and BD Perm2 Buffer, according to manufacturer's instructions.
Instrument	Samples were measured on a MACSQuant® Analyzer 16 and the instrument performance monitored daily with Rainbow Calibration Particles (BD).
Software	Miltenyi MACSquantif software (v2.13) and FlowJo (v9.9.6)
Cell population abundance	Cells have not been enriched or sorted. Data are shown within ex vivo stimulated peripheral blood mononuclear cells.
Gating strategy	All recorded events were gated according to FSC and SSC as lymphocytes; single cells were further selected using FSC-H vs. FSC-W and again using SSC-H vs. SSC-W. Subsequently living cells were identified as ZombieYellow negative cells gated against CD4-BV605. An artefact population in some samples (probably induced by DMSO) was observed disturbing data analysis and was gated out using V500 vs V450. The subsequent gating scheme is depicted in Fig.2a and Fig. 3a.

☒ Tick this box to confirm that a figure exemplifying the gating strategy is provided in the Supplementary Information.